Analysis of a Three-Dimensional Crack Terminating at an Interface Using a Hypersingular Integral Equation Method

T. Y. Qin
College of Engineering Science,
China Agricultural University,
Beijing 100083, P. R. China
e-mail: mech@maile.cau.edu.cn

N. A. Noda
Department of Mechanical Engineering,
Kyushu Institute of Technology,
Kitakyushu 804-8550, Japan

Using a body force method and the finite-part integral concepts, a set of hypersingular integral equations for a vertical crack terminating at an interface in a three-dimensional infinite bimaterial subjected to arbitrary loads are derived. The stress singularity orders and singular stress fields around the crack front terminating at the interface are obtained by the main-part analytical method of hypersingular integral equations. Then, a numerical method for the solution of the hypersingular integral equations in case of a rectangular crack is proposed, in which the crack displacement discontinuities are approximated by the product of basic density functions and polynomials. Numerical solutions for the stress intensity factors of some examples are given. [DOI: 10.1115/1.1488938]

1 Introduction

In recent decades, the use of new materials has been increasing in a wide range of engineering fields and the accurate evaluation of interface strength in dissimilar materials has become very important. Considerable research has been done to evaluate the stress intensity factors and crack-opening displacement for cracks in dissimilar materials ([1–4]). However, most of these works are on two-dimensional cases. Due to the mathematical difficulties, there are not any analytical methods for three-dimensional crack problems. However, several numerical methods are available ([5–8]). Lee and Keer [3] evaluated the stress intensity factors of a crack meeting the interface by a body force method, but they didn't give the singular stress field, and consider the singularity near the crack front at the interface in their numerical method. Noda et al. [9] studied mixed-mode stress intensity factors of an inclined semi-elliptical surface crack by a body force method, in which the unknown body force densities were approximated by the products of fundamental density functions and polynomials. This numerical method was applied by Wang and Noda [10] to investigate the stress intensity factors of a three-dimensional rectangular crack using the body force method.

In the present paper, the hypersingular integral equation method based on the body force method is applied to solve the problem of a three-dimensional vertical crack terminating at an interface, and the stress singularities and singular stress field around the crack front terminating at the interface are obtained by the main-part analytical method of singular integral equations. Based on these theoretical solutions, the numerical approach suggested by Noda and Kobayashi [9] will be used to obtain highly reliable numerical results of stress intensity factors.

2 General Solutions and the Hypersingular Integral Equation for a Planar Crack Meeting the Bimaterial Interface

A fixed rectangular Cartesian system x_i $(i=1,2,3)$ is used. Consider two dissimilar half-spaces bonded together along the x_1-x_3–plane. Suppose that the right half-space (x_2-plane) is occupied by an elastic medium with elastic constants (μ_1,ν_1) and the left half-space ($-x_2$-plane) is occupied by an elastic medium with elastic constants (μ_2,ν_2). The crack is assumed to be in a plane normal to the x_3-axis (Fig. 1). Based on the body force method ([3]), the displacements at a point $\mathbf{x}$ in the materials can be expressed as

$$u_k(\mathbf{x})=\int_S T_{ki}(\mathbf{x},\boldsymbol{\xi})\bar{u}_i(\boldsymbol{\xi})ds(\boldsymbol{\xi}) \quad i,k=1,2,3 \tag{1}$$

where $\bar{u}_i=u_i^+-u_i^-$ is the ith displacement discontinuity of the crack surface, and

$$T_{ki}(\mathbf{x},\boldsymbol{\xi})=\left\{\frac{2\mu_1\nu_1}{1-2\nu_1}\frac{\partial G_{kj}(\mathbf{x},\boldsymbol{\xi})}{\partial\xi_j}\delta_{3i}+\mu_1\times\left[\frac{\partial G_{ki}(\mathbf{x},\boldsymbol{\xi})}{\partial\xi_3}+\frac{\partial G_{k3}(\mathbf{x},\boldsymbol{\xi})}{\partial\xi_i}\right]\right\}_{\xi_3=0}$$
$$j=1,2,3 \tag{2}$$

in which $G_{ij}(\mathbf{x},\boldsymbol{\xi})$ is the Green's function ([3,11]), which represents the x_i-direction displacement at point $\mathbf{x}$ produced by a unit load applied at point $\boldsymbol{\xi}$ in the x_j-direction. Then, the corresponding stress field can be obtained by use of the constitutive relations. The stresses at a point $\mathbf{x}$ outside of crack surface S are written as follows:

$$\sigma_{ij}(\mathbf{x})=\int_S S_{kij}(\mathbf{x},\boldsymbol{\xi})\bar{u}_k(\boldsymbol{\xi})ds(\boldsymbol{\xi}) \tag{3}$$

where

$$S_{kij}(\mathbf{x},\boldsymbol{\xi})=\frac{2\mu_1\nu_1}{1-2\nu_1}\frac{\partial T_{lk}(\mathbf{x},\boldsymbol{\xi})}{\partial x_l}\delta_{ij}+\mu_1\times\left[\frac{\partial T_{ik}(\mathbf{x},\boldsymbol{\xi})}{\partial x_j}+\frac{\partial T_{jk}(\mathbf{x},\boldsymbol{\xi})}{\partial x_i}\right]$$
$$l=1,2,3. \tag{4}$$

The traction boundary conditions of the crack surface are

$$\sigma_{3i}^+(\mathbf{x})=-p_i(\mathbf{x}) \quad \mathbf{x}\in S. \tag{5}$$

Contributed by the Applied Mechanics Division of THE AMERICAN SOCIETY OF MECHANICAL ENGINEERS for publication in the ASME JOURNAL OF APPLIED MECHANICS. Manuscript received by the Applied Mechanics Division, June 20, 2001; final revision, November 5, 2001. Associate Editor: J. R. Barber. Discussion on the paper should be addressed to the Editor, Prof. Robert M. McMeeking, Chair, Department of Mechanics and Environmental Engineering, University of California–Santa Barbara, Santa Barbara, CA 93106-5070, and will be accepted until four months after final publication in the paper itself in the ASME JOURNAL OF APPLIED MECHANICS.

Here the superscript + refers to the upper surface of the crack, and $p_i(\mathbf{x})$ represents the loading on the crack surface due to internal pressure or external loading, and it can obtained from the solution for the loading of the uncracked solid. Using boundary condition (5) and the finite-part integral concepts, the hypersingular integral equations for unknown displacement discontinuities can be obtained:

$$\frac{\mu_1}{\pi(\kappa_1+1)} \oint\!\!\!\!\!\!= \int_S \left[\frac{\kappa_1-1}{2r_1^3}\delta_{\alpha\beta} + \frac{3(3-\kappa_1)}{4r_1^3} r_{1,\alpha} r_{1,\beta} + K_{\alpha\beta}(\mathbf{x},\boldsymbol{\xi}) \right] \bar{u}_\beta(\boldsymbol{\xi}) ds(\boldsymbol{\xi}) = -p_\alpha(\mathbf{x}) \quad \alpha,\beta=1,2 \quad \mathbf{x}\in S \tag{6}$$

$$\frac{\mu_1}{\pi(\kappa_1+1)} \oint\!\!\!\!\!\!= \int_S \left[\frac{1}{r_1^3} + K_0(\mathbf{x},\boldsymbol{\xi}) \right] \bar{u}_3(\boldsymbol{\xi}) ds(\boldsymbol{\xi}) = -p_3(\mathbf{x}) \quad \mathbf{x}\in S \tag{7}$$

where $\oint\!\!\!\!\!\!=$ is the symbol of the finite-part integral, r_1 is the distance from point $\mathbf{x}(x_1,x_2,0)$ to point $\boldsymbol{\xi}(\xi_1,\xi_2,0)$, r_2 is the distance from point $\mathbf{x}(x_1,x_2,0)$ to a symmetric point $(\xi_1,-\xi_2,0)$ of point $\boldsymbol{\xi}$, and

$$K_{11}(\mathbf{x},\boldsymbol{\xi}) = \frac{2A\kappa_1(\kappa_1+6)+2B-5C}{4r_2^3} - \frac{24Ax_2\xi_2}{r_2^5} - \frac{3(4A\kappa_1-C)(x_2+\xi_2)^2}{4r_2^5} + \frac{30Ax_2\xi_2(x_2+\xi_2)^2}{r_2^7} - \frac{3(2A\kappa_1+A\kappa_1^2+B-2C)}{2r_2r_3^2} \tag{8}$$

$$K_{12}(\mathbf{x},\boldsymbol{\xi}) = (x_1-\xi_1)\left[\frac{3C(x_2+\xi_2)}{4r_2^5} + \frac{30Ax_2\xi_2(x_2+\xi_2)}{r_2^7} + \frac{3A(\kappa_1-1)x_2}{r_2^5} + \frac{1}{2}(A\kappa_1+B-C) \times \left(\frac{1}{r_2^2r_3^2} + \frac{1}{r_2^3r_3} \right) \right] \tag{9}$$

$$K_{21}(\mathbf{x},\boldsymbol{\xi}) = (x_1-\xi_1) \times \left[\frac{3(4A+4A\kappa_1-C)(x_2+\xi_2)}{4r_2^5} + \frac{3A(\kappa_1-1)x_2}{r_2^5} - \frac{30Ax_2\xi_2(x_2+\xi_2)}{r_2^7} - \frac{1}{2}(A\kappa_1+B-C) \times \left(\frac{1}{r_2^2r_3^2} + \frac{1}{r_2^3r_3} \right) \right] \tag{10}$$

$$K_{22}(\mathbf{x},\boldsymbol{\xi}) = \frac{A+B-C}{2r_2^3} + \frac{3(C-4A)(x_2+\xi_2)^2}{4r_2^5} + \frac{24Ax_2\xi_2}{r_2^5} - \frac{30Ax_2\xi_2(x_1-\xi_1)^2}{r_2^7} \tag{11}$$

$$K_0(\mathbf{x},\boldsymbol{\xi}) = \frac{2C-3A(\kappa_1^2-2\kappa_1+3)}{2r_2^3} + \frac{3A[12x_2\xi_2-(3-\kappa_1)(\kappa_1-1)(x_2+\xi_2)^2]}{2r_2^5} + \frac{3(2A\kappa_1+A\kappa_1^2+B-2C)}{2r_2r_3^2} \tag{12}$$

and

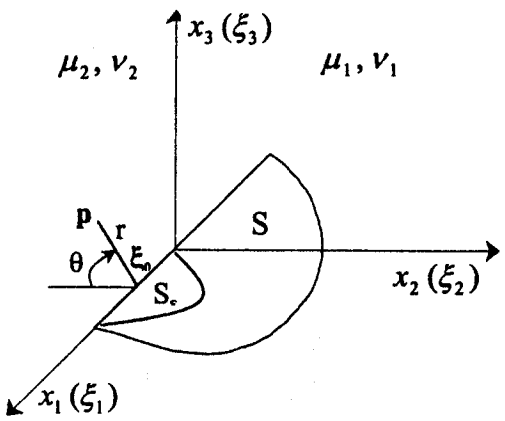

Fig. 1 Problem configuration

$$r_1=\sqrt{(x_1-\xi_1)^2+(x_2-\xi_2)^2}, \quad r_2=\sqrt{(x_1-\xi_1)^2+(x_2+\xi_2)^2},$$
$$r_3=r_2+x_2+\xi_2,$$
$$r_{1,\alpha}=(\xi_\alpha-x_\alpha)/r_1, \quad A=(\mu_1-\mu_2)/(\mu_1+\kappa_1\mu_2),$$
$$B=(\kappa_2\mu_1-\kappa_1\mu_2)/(\mu_2+\kappa_2\mu_1).$$
$$S=(\mu_1-\mu_2)/(\mu_1+\mu_2), \quad C=S(\kappa_1+1),$$
$$\kappa_1=3-4\nu_1, \quad \kappa_2=3-4\nu_2.$$

Equation (7) is the same as that given by Lee and Keer [3].

3 Stress Singularity Near the Crack Front at the Interface

According to the elastic theory [12], the displacement discontinuities of the crack surface near a point $\boldsymbol{\xi}_0$ at the interface can be assumed as

$$\bar{u}_k(\boldsymbol{\xi}) = D_k(\boldsymbol{\xi}_0)\xi_2^{\lambda_k} \quad 0<\mathrm{Re}(\lambda_k)<1 \quad k=1,2,3 \tag{13}$$

where $D_k(\boldsymbol{\xi}_0)$ is a nonzero constant related to point $\boldsymbol{\xi}_0$, and λ_k is the stress singular index near the crack front meeting the interface. Consider a small semicircle domain S_ε on the crack surface including point $\boldsymbol{\xi}_0$ as shown in Fig. 1. Let $t=\xi_2/x_2$, $\eta=\xi_1/x_2$, $x_1=x_2\mathrm{ctg}\varphi$, and $x_2\to 0$, and using the main-part analytical method ([12,13]), the following relations can be derived:

$$\oint\!\!\!\!\!\!= \int_{S_\varepsilon} \frac{\bar{u}_1}{r_1^3} d\xi_1 d\xi_2 = D_1(\boldsymbol{\xi}_0)x_2^{\lambda_1-1} \oint\!\!\!\!\!\!= \int_0^\infty t^{\lambda_1} dt \times \int_{-\infty}^{\infty} \frac{d\eta}{[(\eta-\mathrm{ctg}\varphi)^2+(1-t)^2]^{3/2}} \cong -2\pi\lambda_1 D_1(\boldsymbol{\xi}_0)x_2^{\lambda_1-1}\cot(\lambda_1\pi) \tag{14}$$

$$\oint\!\!\!\!\!\!= \int_{S_\varepsilon} \frac{(x_1-\xi_1)^2}{r_1^5} \bar{u}_1 d\xi_1 d\xi_2 \cong -\frac{2}{3}\pi\lambda_1 D_1(\boldsymbol{\xi}_0)x_2^{\lambda_1-1}\cot(\lambda_1\pi) \tag{15}$$

$$\int_{S_\varepsilon} \frac{\bar{u}_2}{r_2^3} d\xi_1 d\xi_2 \cong 2\pi\lambda_2 D_2(\boldsymbol{\xi}_0)x_2^{\lambda_2-1}\frac{1}{\sin(\lambda_2\pi)} \tag{16}$$

$$\int_{S_\varepsilon} \frac{x_2\xi_2}{r_2^5} \bar{u}_2 d\xi_1 d\xi_2 \cong \frac{2}{9}\pi\lambda_2(1-\lambda_2^2) D_2(\boldsymbol{\xi}_0)x_2^{\lambda_2-1}\frac{1}{\sin(\lambda_2\pi)} \tag{17}$$

$$f^1_{332}(\theta)=\frac{1}{\omega}\{-2(1-\lambda)\sin\theta\cos(2-\lambda)\theta+[2A\kappa_1-3A+B+2A\gamma(1+\lambda)+2A(1-\lambda)(2+\lambda)]\sin(\lambda\pi+\theta-\lambda\theta)+2A(1-\lambda)(2+\gamma+\lambda)\sin(\lambda\pi+3\theta-\lambda\theta)\} \quad (42)$$

and here $\omega=[2-A-B-2\lambda(A-B)]$, $\gamma=(3-\kappa_1)/2(\kappa_1-1)$. The superscript 1 refers to the material 1 marked in Fig. 1.

For a point $\mathbf{p}$ near the crack front in the material 2, using the following relations:

$$\int_{S_\varepsilon}\left(\frac{1}{r_1^3}-\frac{3x_3^2}{r_1^5}\right)\bar{u}_3 d\xi_1 d\xi_2\cong\frac{2\pi\lambda D_3(\xi_0)r^{\lambda-1}}{\sin(\lambda\pi)}\cos(1-\lambda)\theta \quad (43)$$

$$\int_{S_\varepsilon}\frac{1}{2}x_3\left(\frac{3}{r_1^2r_4^2}+\frac{3}{r_1^3r_4}-\frac{2x_3^2}{r_1^3r_4^3}-\frac{3x_3^2}{r_1^4r_4^2}-\frac{3x_3^2}{r_1^5r_4}\right)\bar{u}_2 d\xi_1 d\xi_2\cong\frac{2\pi\lambda D_2(\xi_0)r^{\lambda-1}\sin(1-\lambda)\theta}{\sin\lambda\pi} \quad (44)$$

$$\int_{S_\varepsilon}\left[\frac{3}{r_1r_4^2}-\frac{6x_3^2}{r_1^3r_4^2}-\frac{12x_3^2}{r_1^2r_4^3}+\frac{6x_3^4}{r_1^3r_4^4}+\frac{6x_3^4}{r_1^4r_4^3}+\frac{3x_3^4}{r_1^5r_4^2}\right]\bar{u}_3 d\xi_1 d\xi_2\cong\frac{2\pi\lambda D_3(\xi_0)r^{\lambda-1}\cos(1-\lambda)\theta}{\sin\lambda\pi} \quad (45)$$

$$\int_{S_\varepsilon}\left[\frac{3}{r_1^3r_4}+\frac{3}{r_1^2r_4^2}-\frac{18x_3^2}{r_1^5r_4}-\frac{18x_3^2}{r_1^4r_4^2}-\frac{12x_3^2}{r_1^3r_4^3}+\frac{15x_3^4}{r_1^7r_4}+\frac{15x_3^4}{r_1^6r_4^2}+\frac{12x_3^4}{r_1^5r_4^3}+\frac{6x_3^4}{r_1^4r_4^4}\right]\bar{u}_3 d\xi_1 d\xi_2\cong-\frac{\pi\lambda(1-\lambda)D_3(\xi_0)r^{\lambda-1}}{\sin\lambda\pi}[\cos(1-\lambda)\theta+\cos(3-\lambda)\theta] \quad (46)$$

$$\int_{S_\varepsilon}\frac{(x_2-\xi_2)x_3\bar{u}_2}{r_1^5}d\xi_1 d\xi_2\cong-\frac{2\pi\lambda D_2(\xi_0)r^{\lambda-1}}{3\sin(\lambda\pi)}\sin(1-\lambda)\theta \quad (47)$$

$$\int_{S_\varepsilon}\frac{(x_2-\xi_2)x_3^3}{r_1^7}\bar{u}_2 d\xi_1 d\xi_2\cong\frac{\pi\lambda D_2(\xi_0)r^{\lambda-1}}{15\sin(\lambda\pi)}[-(3-\lambda)\sin(1-\lambda)\theta+(1-\lambda)\sin(3-\lambda)\theta] \quad (48)$$

$$\int_{S_\varepsilon}x_3\left(\frac{3}{r_1^2r_4^2}+\frac{3}{r_1^3r_4}-\frac{2x_3^2}{r_1^3r_4^3}-\frac{3x_3^2}{r_1^4r_4^2}-\frac{3x_3^2}{r_1^5r_4}\right)\bar{u}_2 d\xi_1 d\xi_2\cong\frac{2\pi\lambda D_2(\xi_0)r^{\lambda-1}\sin(1-\lambda)\theta}{\sin\lambda\pi} \quad (49)$$

where $r_4=r_2-x_2+\xi_2$, the singular stresses can be expressed by

$$\sigma^2_{13}(\mathbf{p})=-\frac{\mu_1\mu_2\lambda_1 D_1(\xi_0)}{(\mu_1+\mu_2)\sin(\lambda_1\pi)r^{1-\lambda_1}}\cos(1-\lambda_1)\theta \quad -\pi/2<\theta\leqslant\pi/2 \quad (50)$$

$$\sigma^2_{23}(\mathbf{p})=\frac{\mu_1\lambda\omega D_3(\xi_0)}{(1+\kappa_1)\sin(\lambda\pi)r^{1-\lambda}}f^2_{231}(\theta)+\frac{\mu_1\lambda\omega D_2(\xi_0)}{(1+\kappa_1)\sin(\lambda\pi)r^{1-\lambda}}f^2_{232}(\theta) \quad -\pi/2<\theta\leqslant\pi/2 \quad (51)$$

$$\sigma^2_{33}(\mathbf{p})=\frac{\mu_1\lambda\omega D_3(\xi_0)}{(1+\kappa_1)\sin(\lambda\pi)r^{1-\lambda}}f^2_{331}(\theta)+\frac{\mu_1\lambda\omega D_2(\xi_0)}{(1+\kappa_1)\sin(\lambda\pi)r^{1-\lambda}}f^2_{332}(\theta) \quad -\pi/2<\theta\leqslant\pi/2 \quad (52)$$

$$f^2_{231}(\theta)=\frac{1}{\omega}\{[\Gamma(\kappa_1+B)-(1-A)(\kappa_1-1)-\lambda(1-2A+B)]\sin(1-\lambda)\theta-(1-\lambda)(1-B)\sin(3-\lambda)\theta\} \quad (53)$$

$$f^2_{232}(\theta)=-\frac{1}{\omega}2(1-\lambda)(1-B)\sin\theta\sin(2-\lambda)\theta+\cos(1-\lambda)\theta \quad (54)$$

$$f^2_{331}(\theta)=-\frac{1}{\omega}2(1-\lambda)(B-1)\sin\theta\sin(2-\lambda)\theta+\cos(1-\lambda)\theta \quad (55)$$

$$f^2_{332}(\theta)=\frac{1}{\omega}[(A-2B+1+2A\lambda-B\lambda-\lambda)\sin(1-\lambda)\theta-(1-B)(1-\lambda)\sin(3-\lambda)\theta]. \quad (56)$$

Here the superscript 2 refers to the material 2 marked in Fig. 1. Other singular stresses near point ξ_0 can also be obtained by use of the above method. Using definitions (24)–(26), relation (13) and solutions (50)–(52), the stress intensity factors at the crack front on the interface can be written as

$$K_{\mathrm{I}}=\frac{2^{1-\lambda}\mu_1\lambda\omega D_3(\xi_0)}{(1+\kappa_1)\sin(\lambda\pi)}=\lim_{\xi_2\to0}\frac{2^{1-\lambda}\lambda\mu_1\omega\bar{u}_3}{(\kappa_1+1)\sin\lambda\pi\xi_2^\lambda} \quad (57)$$

$$K_{\mathrm{II}}=\frac{2^{1-\lambda}\mu_1\lambda\omega D_2(\xi_0)}{(1+\kappa_1)\sin(\lambda\pi)}=\lim_{\xi_2\to0}\frac{2^{1-\lambda}\lambda\mu_1\omega\bar{u}_2}{(\kappa_1+1)\sin\lambda\pi\xi_2^\lambda} \quad (58)$$

$$K_{\mathrm{III}}=\frac{2^{1-\lambda_1}\mu_1\mu_2\lambda_1 D_1(\xi_0)}{(\mu_1+\mu_2)\sin(\lambda_1\pi)}=\lim_{\xi_2\to0}\frac{2^{1-\lambda_1}\mu_1\mu_2\bar{u}_1}{(\mu_1+\mu_2)\sin(\lambda_1\pi)\xi_2^{\lambda_1}}. \quad (59)$$

Using relations (56)–(59), the singular stresses solutions (40), (50)–(52) are expressed:

$$\sigma^1_{33}=\frac{K_{\mathrm{I}}}{(2r)^{1-\lambda}}f^1_{331}(\theta)+\frac{K_{\mathrm{II}}}{(2r)^{1-\lambda}}f^1_{332}(\theta) \quad \pi/2\leqslant|\theta|\leqslant\pi \quad (60)$$

$$\sigma^2_{13}=-\frac{K_{\mathrm{III}}}{(2r)^{1-\lambda_1}}\cos(1-\lambda_1)\theta \quad -\pi/2<\theta\leqslant\pi/2 \quad (61)$$

$$\sigma^2_{23}=\frac{K_{\mathrm{I}}}{(2r)^{1-\lambda}}f^2_{231}(\theta)+\frac{K_{\mathrm{II}}}{(2r)^{1-\lambda}}f^2_{232}(\theta) \quad -\pi/2<\theta\leqslant\pi/2 \quad (62)$$

$$\sigma^2_{33}=\frac{K_{\mathrm{I}}}{(2r)^{1-\lambda}}f^2_{331}(\theta)+\frac{K_{\mathrm{II}}}{(2r)^{1-\lambda}}f^2_{332}(\theta) \quad -\pi/2<\theta\leqslant\pi/2. \quad (63)$$

In the case of homogeneity, solutions (60)–(63) are the same as that given by Tang and Qin [13].

5 Numerical Procedure

Consider a rectangular crack meeting the interface in a three-dimensional infinite elastic solid under a normal load as shown in Fig. 2. Using its known behavior near the crack front and the fundamental solutions, the crack-opening displacement can be written as

$$\int_{S_\varepsilon}\frac{(x_2+\xi_2)^2}{r_2^5}\bar{u}_2 d\xi_1 d\xi_2 \cong \frac{4}{3}\pi\lambda_2 D_2(\xi_0)x_2^{\lambda_2-1}\frac{1}{\sin(\lambda_2\pi)} \tag{18}$$

$$\int_{S_\varepsilon}\frac{x_2\xi_2(x_1-\xi_1)^2}{r_2^7}\bar{u}_2 d\xi_1 d\xi_2 \cong \frac{8}{45}\pi\lambda_2(1-\lambda_2^2)D_2(\xi_0)x_2^{\lambda_2-1}\frac{1}{\sin(\lambda_2\pi)} \tag{19}$$

$$\int_{S_\varepsilon}\frac{x_2\xi_2(x_2+\xi_2)^2}{r_2^7}\bar{u}_1 d\xi_1 d\xi_2 \cong \frac{2}{45}\pi\lambda_1(1-\lambda_1^2)D_1(\xi_0)x_2^{\lambda_1-1}\frac{1}{\sin(\lambda_1\pi)} \tag{20}$$

$$\int_{S_\varepsilon}\frac{\bar{u}_3}{r_2 r_3^2}d\xi_1 d\xi_2 \cong \frac{2}{3}\pi\lambda_3 D_3(\xi_0)x_2^{\lambda_3-1}\frac{1}{\sin(\lambda_3\pi)}. \tag{21}$$

Using the above relations, from Eqs. (6) and (7), the stress singular index can be obtained. It can be shown than $\lambda_2=\lambda_3=\lambda$, and

$$4A\lambda^2+2\cos(\lambda\pi)-A-B=0 \tag{22}$$

$$\cos(\lambda_1\pi)=S. \tag{23}$$

The characteristic Eq. (22) is coincident with that for the two-dimensional case ([1,4]), and (23) is coincident with that for the antiplane case ([2]). The stress intensity factors at the crack front on the interface are defined by

$$K_1=\lim_{r\to 0}\sigma_{33}(r,\theta)_{|\theta=0}(2r)^{1-\lambda} \tag{24}$$

$$K_{11}=\lim_{r\to 0}\sigma_{23}(r,\theta)_{|\theta=0}(2r)^{1-\lambda} \tag{25}$$

$$K_{111}=\lim_{r\to 0}\sigma_{13}(r,\theta)_{|\theta=0}(2r)^{1-\lambda_1}. \tag{26}$$

4 Singular Stress Field Near the Crack Front at the Interface

Based on relation (13), the singular stress field around the crack front terminating at the interface can be obtained by the main-part analytical method. For a point **p** near the crack front in the material 1, using following relations:

$$\int_{S_\varepsilon}\left(\frac{1}{r_1^3}+\frac{6x_3^2}{r_1^5}-\frac{15x_3^4}{r_1^7}\right)\bar{u}_3 d\xi_1 d\xi_2 \cong \frac{2\pi\lambda(1-\lambda)D_3(\xi_0)r^{\lambda-1}}{\sin(\lambda\pi)} \times\sin\theta\sin(2-\lambda)\theta \tag{27}$$

$$\int_{S_\varepsilon}\frac{\bar{u}_3}{r_2^3}d\xi_1 d\xi_2 \cong \frac{2\pi D_3(\xi_0)r^{\lambda-1}\sin\lambda(\pi-\theta)}{\sin(\lambda\pi)\sin\theta} \tag{28}$$

$$\int_{S_\varepsilon}\frac{(x_2+\xi_2)^2\bar{u}_3}{r_2^5}d\xi_1 d\xi_2 \cong \frac{2\pi D_3(\xi_0)r^{\lambda-1}}{3\sin(\lambda\pi)\sin\theta}[\sin\lambda(\pi-\theta) -\lambda\sin\theta\cos(\lambda\pi+\theta-\lambda\theta)] \tag{29}$$

$$\int_{S_\varepsilon}\left(\frac{12x_3^2}{r_2^5}-\frac{15x_3^4}{r_2^7}-\frac{15(x_2+\xi_2)^2x_3^2}{r_2^7}\right)\bar{u}_3 d\xi_1 d\xi_2 \cong 0 \tag{30}$$

$$\int_{S_\varepsilon}\left(\frac{18x_2\xi_2}{r_2^5}-\frac{180x_2\xi_2x_3^2}{r_2^7}+\frac{210x_2\xi_2x_2^4}{r_2^9}\right)\bar{u}_3 d\xi_1 d\xi_2 \cong \frac{4\pi\lambda(1-\lambda^2)D_3(\xi_0)r^{\lambda-1}\cos\theta\cos(\lambda\pi+2\theta-\lambda\theta)}{\sin(\lambda\pi)} \tag{31}$$

$$\int_{S_\varepsilon}\left(\frac{3}{r_2r_3^2}-\frac{6x_3^2}{r_2^3r_3^2}-\frac{12x_3^2}{r_2^2r_3^3}+\frac{6x_3^4}{r_2^3r_3^4}+\frac{6x_3^4}{r_2^4r_3^3}+\frac{3x_3^4}{r_2^5r_3^2}\right)\bar{u}_3 d\xi_1 d\xi_2 \cong -\frac{2\pi\lambda D_3(\xi_0)r^{\lambda-1}\cos(\lambda\pi+\theta-\lambda\theta)}{\sin\lambda\pi} \tag{32}$$

$$\int_{S_\varepsilon}(x_2-\xi_2)x_3\left(\frac{3}{r_1^5}-\frac{15x_3^2}{r_1^7}\right)\bar{u}_2 d\xi_1 d\xi_2 \cong -\frac{2\pi\lambda(1-\lambda)D_2(\xi_0)r^{\lambda-1}}{\sin(\lambda\pi)}\sin\theta\cos(2-\lambda)\theta \tag{33}$$

$$\int_{S_\varepsilon}\frac{(x_2+\xi_2)x_3\bar{u}_2}{r_2^5}d\xi_1 d\xi_2 \cong \frac{2\pi\lambda D_2(\xi_0)r^{\lambda-1}}{3\sin(\lambda\pi)}\sin(\lambda\pi+\theta-\lambda\theta) \tag{34}$$

$$\int_{S_\varepsilon}\frac{x_2x_3\bar{u}_2}{r_2^5}d\xi_1 d\xi_2 \cong -\frac{2\pi\lambda D_2(\xi_0)r^{\lambda-1}\cos\theta}{3\sin(\lambda\pi)\sin^2\theta}[\sin(\lambda\pi-\lambda\theta) +\lambda\sin\theta\cos(\lambda\pi+\theta-\lambda\theta)] \tag{35}$$

$$\int_{S_\varepsilon}\frac{x_2x_3^3\bar{u}_2}{r_2^7}d\xi_1 d\xi_2 \cong -\frac{2\pi\lambda D_2(\xi_0)r^{\lambda-1}\cos\theta}{3\sin(\lambda\pi)\sin^2\theta}[3\sin\lambda(\pi-\lambda\theta) +3\lambda\sin\theta\cos(\lambda\pi+\theta-\lambda\theta) +\lambda(1-\lambda)\sin^2\theta\sin(\lambda\pi+2\theta-\lambda\theta)] \tag{36}$$

$$\int_{S_\varepsilon}\frac{x_3(x_2+\xi_2)^3\bar{u}_2}{r_2^7}d\xi_1 d\xi_2 \cong \frac{2\pi\lambda D_2(\xi_0)r^{\lambda-1}}{15\sin(\lambda\pi)}[3\sin(\lambda\pi+\theta -\lambda\theta)+(1-\lambda)\sin\theta\cos(\lambda\pi+2\theta -\lambda\theta)] \tag{37}$$

$$\int_{S_\varepsilon}x_2\xi_2(x_2+\xi_2)x_3\left(\frac{90}{r_2^7}-\frac{210x_3^2}{r_2^9}\right)\bar{u}_2 d\xi_1 d\xi_2 \cong \frac{4\pi\lambda(1-\lambda^2)D_2(\xi_0)r^{\lambda-1}\cos\theta\sin(\lambda\pi+2\theta-\lambda\theta)}{\sin(\lambda\pi)} \tag{38}$$

$$\int_{S_\varepsilon}\frac{1}{2}x_3\left(\frac{3}{r_2^2r_3^2}+\frac{3}{r_2^3r_3}-\frac{2x_3^2}{r_2^3r_3^3}-\frac{3x_3^2}{r_2^4r_3^2}-\frac{3x_3^2}{r_2^5r_3}\right)\bar{u}_2 d\xi_1 d\xi_2 \cong -\frac{2\pi\lambda D_2(\xi_0)r^{\lambda-1}\cos(\lambda\pi+\theta-\lambda\theta)}{\sin\lambda\pi} \tag{39}$$

here r_1 is the distance from point $\mathbf{p}(x_1,x_2,x_3)$ to point $\xi(\xi_1,\xi_2,0)$ and r_2 is the distance from point $\mathbf{p}(x_1,x_2,x_3)$ to the symmetric point $(\xi_1,-\xi_2,0)$ of point $\xi(\xi_1,\xi_2,0)$, e.g., $r_1=\sqrt{(x_1-\xi_1)^2+(x_2-\xi_2)^2+x_3^2}$, $r_2=\sqrt{(x_1-\xi_1)^2+(x_2+\xi_2)^2+x_3^2}$, $r_3=r_2+x_2+\xi_2$, from (3), the singular stress can be expressed by

$$\sigma_{33}^1(\mathbf{p})=\frac{\mu_1\lambda\omega D_3(\xi_0)}{(1+\kappa_1)\sin(\lambda\pi)r^{1-\lambda}}f_{331}^1(\theta) +\frac{\mu_1\lambda\omega D_2(\xi_0)}{(1+\kappa_1)\sin(\lambda\pi)r^{1-\lambda}}f_{332}^1(\theta)\quad \pi/2\leqslant|\theta|\leqslant\pi \tag{40}$$

$$f_{331}^1(\theta)=\frac{1}{\omega}\{2\cos(1-\lambda)\theta+2(1-\lambda)\sin\theta\sin(2-\lambda)\theta +[A(1-2\lambda)(2+\lambda)+B]\cos(\lambda\pi+\theta-\lambda\theta)+A(1-\lambda) \times(1-2\lambda)\cos(\lambda\pi+3\theta-\lambda\theta)\} \tag{41}$$

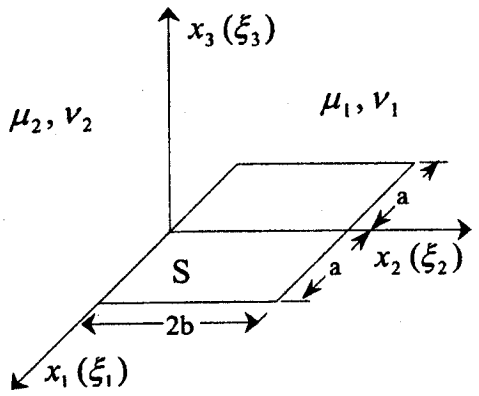

Fig. 2 A rectangular crack meeting the interface

$$\tilde{u}_3(\xi_1,\xi_2)=F_3(\xi_1,\xi_2)\xi_2^{\lambda}\sqrt{(a^2-\xi_1^2)(2b-\xi_2)}. \tag{64}$$

To numerically solve the unknown function $\tilde{u}_3$, the unknown function $F_i(\xi_1,\xi_2)$ is assumed as

$$F_3(\xi_1,\xi_2)=\sum_{n=1}^{N} a_{3n}G_n(\xi_1,\xi_2) \tag{65}$$

where a_{3n} is unknown constants $N=(K+1)(L+1)$, and

$$G_1(\xi_1,\xi_2)=1,\quad G_2(\xi_1,\xi_2)=\xi_1,\ \ldots,$$
$$G_{K+1}(\xi_1,\xi_2)=\xi_1^K,\quad G_{K+2}(\xi_1,\xi_2)=\xi_2,$$
$$G_{K+3}(\xi_1,\xi_2)=\xi_1\xi_2,\ \ldots,\quad G_{2K+2}(\xi_1,\xi_2)=\xi_1^K\xi_2,\ \ldots,$$
$$G_{(K+1)(L+1)}(\xi_1,\xi_2)=\xi_1^K\xi_2^L. \tag{66}$$

Substituting (64) and (65) into (7), a set of algebraic linear equations for unknown a_{3n} can be obtained:

$$\sum_{n=1}^{N} a_{3n}[I_{3n}^1(x_1,x_2)+I_{3n}^2(x_1,x_2)]=-\frac{\pi(\kappa_1+1)}{\mu_1}p_3(x_1,x_2) \tag{67}$$

where

$$I_{3n}^1(x_1,x_2)=\oint\!\!\!\!\!\!-_S \frac{1}{r_1^3}\omega_2(\xi_1,\xi_2)d\xi_1 d\xi_2 \tag{68}$$

$$I_{3n}^2(x_1,x_2)=\int_S K_0(\mathbf{x},\boldsymbol{\xi})\omega_2(\xi_1,\xi_2)d\xi_1 d\xi_2 \tag{69}$$

in which

$$\omega_2(\xi_1,\xi_2)=\xi_2^{\lambda}\sqrt{(a^2-\xi_1^2)(2b-\xi_2)}G_n(\xi_1,\xi_2). \tag{70}$$

Integral (69) is general one, and can be numerically calculated. Integral (68) is hypersingular one, and must be treated before being numerically evaluated. Using the finite-part integral method ([14]) and the following relations

$$\xi_1=\chi_1+r_1\cos\theta_1\quad \xi_2=x_2+r_1\sin\theta_1 \tag{71}$$

$$\omega_2(\xi_1,\xi_2)=\omega_2(x_1,x_2)+D_{21}(x_1,x_2,\theta_1)r_1 + D_{22}(x_1,x_2,r_1,\theta_1)r_1^2, \tag{72}$$

the hypersingular integral (68) can be written as

$$I_{3n}^1(x_1,x_2)=\int_0^{2\pi}\left[-\frac{\omega_2(x_1,x_2)}{R(\theta_1)}+D_{21}(x_1,x_2,\theta_1)\ln R(\theta_1) + \int_0^{R(\theta_1)} D_{22}(x_1,x_2,r_1,\theta_1)dr_1\right]d\theta \tag{73}$$

where $D_{21}(x_1,x_2,\theta_1)$, and $D_{22}(x_1,x_2,r_1,\theta_1)$ are known functions, and can be derived by the Taylor expansion method. Now the integrals in (73) are generals, and can be calculated numerically. Using the above method, Eq. (6) can also be numerically solved.

6 Numerical Results

In order to verify the above method and illustrate its application, numerical results for a rectangular crack are presented in this section. Consider a rectangular crack meeting the interface in a three-dimensional infinite elastic solid under a uniform tension load σ_{33}^{∞} in infinity as shown in Fig. 2. The dimensionless stress intensity factor of the crack front for mode I is defined as

$$F_1=K_1/\sigma_{33}^{\infty}b^{1-\lambda}. \tag{74}$$

The collocation point number is taken as 20×20 for the present results. Before the results for the general cases are presented, two special cases of a square crack in homogenous materials and surface cracks are compared to other results. In the case of homogeneous materials, the numerical results of the stress intensity factor for a square crack are given in Table 1, and compared with those given by Wang and Noda [10]. It is shown that the results are convergent, and the polynomial exponents $K=L=9$ are enough for a satisfied result precision in this case, and these polynomial exponents will be taken for the following results.

A surface crack corresponds to the limiting case when $\mu_2/\mu_1=0$, and the values of the stress intensity factors at the crack front point (0, $2b$, 0) are given in Table 2. It is shown that present results agree with those by Noda and Wang [15] and Isida and Yoshida [16].

Numerical results for two typical examples are given below. Figure 3 gives the maximum dimensionless stress intensity factors at the center of the crack front on the interface varied with the ratio of μ_2/μ_1 for different ratios of a/b. Obviously, the variations of the stress intensity factors for the cracks with different ratios of a/b are similar, and more gently when $\mu_2/\mu_1\geq 20$. So the material 2 can be treated as a rigid medium when $\mu_2/\mu_1\geq 20$. The dimensionless stress intensity factors along the crack front at the interface are shown in Fig. 4 for different ratios of a/b ($\mu_2/\mu_1=0.5$) and compared with the two-dimensional case. It is shown that the stress intensity factor at the center of the crack front for the case of $a/b\geq 8$ is close to that of the two-dimensional case. This indicates that the stress intensity factor at the center of the crack front for the case of $a/b\geq 8$ can be calculated as the two-dimensional case.

7 Conclusion

A set of hypersingular integral equations of a flat crack terminating at a bimaterial interface in a three-dimensional infinite solid subjected to arbitrary loads is derived. The behaviors of the crack displacement discontinuities near the crack front meeting at the interface are analyzed by the main-part analytical method of hypersingular singular integral equations, and the singular orders are given. Then, the singular stress fields around the crack front terminating at the interface are obtained. Although the expressions of the displacements and stresses in the materials are complex in modality, the analytical solutions of singular stresses around the crack front are brief.

A numerical method for hypersingular integral equations of a rectangular crack terminating at the bimaterial interface is proposed, and the crack displacement discontinuities are approximated by products of a series of power polynomials and fundamental solutions, which exactly express the singularities of stresses near the crack front. This technique should be improved for other shape cracks in the future.

Highly reliable numerical results of stress intensity factors of mode I along the crack front are obtained. The numerical results show that this numerical technique for a rectangular crack is successful, and the solution precision is satisfied. From the numerical

Table 1 Convergence of stress intensity factor F_1 ($x_2=0$, $a/b=1$, $\mu_2/\mu_1=1$, $\nu_1=\nu_2=0.3$, $K=L$)

x_1/a	0/11	1/11	2/11	3/11	4/11	5/11	6/11	7/11	8/11	9/11	10/11
$K=6$	0.7522	0.7505	0.7468	0.7383	0.7260	0.7072	0.6821	0.6506	0.6085	0.5521	0.4446
$K=7$	0.7539	0.7534	0.7487	0.7391	0.7243	0.7046	0.6803	0.6508	0.6122	0.5528	0.4396
$K=8$	0.7512	0.7508	0.7474	0.7396	0.7260	0.7061	0.6803	0.6489	0.6102	0.5536	0.4451
$K=9$	0.7534	0.7512	0.7462	0.7379	0.7255	0.7072	0.6821	0.6497	0.6090	0.5521	0.4464
$K=10$	0.7534	0.7517	0.7465	0.7376	0.7245	0.7065	0.6827	0.6511	0.6088	0.5499	0.4523
$K=11$	0.7533	0.7517	0.7466	0.7377	0.7245	0.7064	0.6827	0.6514	0.6087	0.5491	0.4535
Wang	0.7534	0.7517	0.7465	0.7376	0.7245	0.7066	0.6828	0.6512	0.6086	0.5492	0.4536

Table 2 Dimensionless stress intensity factor F_1 for $\mu_2/\mu_1=0$, $\nu_1=0.3$ at $x_1=0$, $x_2=2b$

a/b	1	2	4	8	10	∞
Present	0.810	1.113	1.387	1.530	1.552	1586
Noda	0.810	1.112	1.386	1.529	1.550	-
Isida	0.803	1.069	1.318	1.481	-	1586

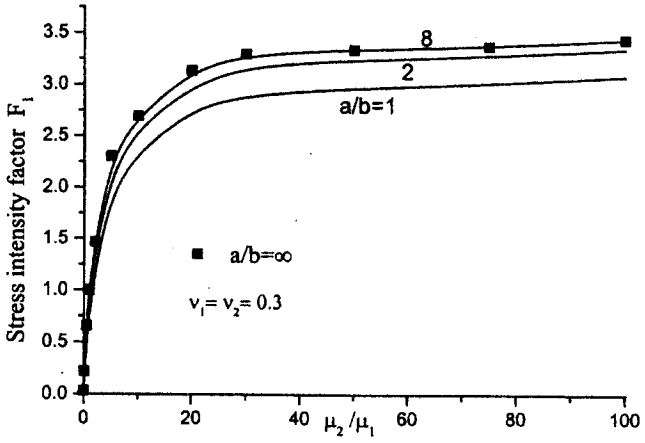

Fig. 3 Stress intensity factor F_1 at the center of the crack front on the interface ($x_2=0$)

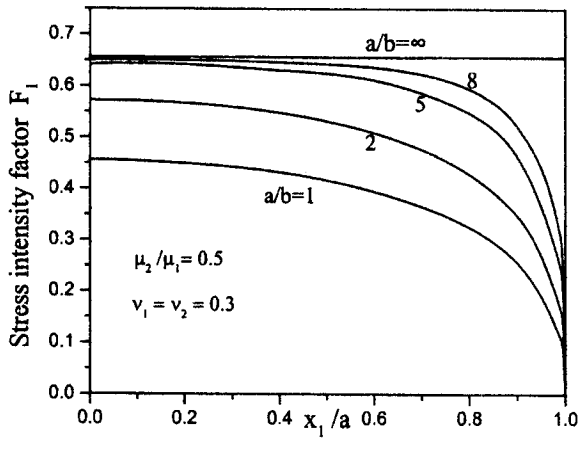

Fig. 4 Stress intensity factor F_1 along the crack front on the interface for $\mu_2/\mu_1=0.5$

solutions, it is shown that the stress intensity factors vary more gently when $\mu_2/\mu_1 \geq 20$, and the material 2 can be treated as a rigid medium in this case. Moreover, the stress intensity factor at the center of the crack front for the case of $a/b \geq 8$ is close to that of the two-dimensional case.

Acknowledgment

Financial supports from the Inoue Foundation for Science and the 75th Commemoration Fund of Kyushu Institute of Technology are gratefully acknowledged.

References

[1] Cook, T. S., and Erdogan, F., 1972, "Stresses in Bonded Materials With a Crack Perpendicular to the Interface," Int. J. Solids Struct., **10**, pp. 677–697.
[2] Erdogan, F., and Cook, T. S., 1974, "Antiplane Shear Crack Terminating at and Going Through a Bimaterial Interface," Int. J. Fract., **10**, pp. 227–240.
[3] Lee, J. C., and Keer, L. M., 1986, "Study of a Three-Dimensional Crack Terminating at an Interface," ASME J. Appl. Mech., **53**, pp. 311–316.
[4] Chen, D. H., and Nisitani, H., 1993, "Stress Intensity Factors of a Crack Meeting the Bimaterial Interface," Trans. Jpn. Soc. Mech. Eng., Ser. A, **59**, pp. 47–53 (in Japanese).
[5] Xu, G., and Ortiz, M., 1993, "A Variational Boundary Integral Method for the Analysis of 3-D Cracks of Arbitrary Geometry Modeled as Continuous Distributions of Dislocation Loops," Int. J. Numer. Methods Eng., **36**, pp. 3675–3701.
[6] Xu, Y., Moran, B., and Belytschko, T., 1997, "Self-Similar Crack Expansion Method for Three-Dimensional Crack Analysis," ASME J. Appl. Mech., **64**, pp. 729–737.
[7] Guo, Q., and Wang, J.-J., et al., 1995, "Elastic Analyses of Planar Cracks Arbitrary Shape," ASME J. Appl. Mech., **62**, pp. 108–115.
[8] Dai, D. N., Hills, D. A., and Nowell, D. N., 1997, "Modeling of Growth of Three-Dimensional Cracks by a Continuous Distribution of Dislocation Loops," Computational Mech., Berlin, **19**, pp. 538–544.
[9] Noda, N. A., Kobayashi, K., and Yagishita, M., 1999, "Variation of Mixed Modes Stress Intensity Factors of an Inclined Semi-Elliptical Surface Cracks," Int. J. Fract., **100**, pp. 207–225.
[10] Wang, Q., et al., 2000, "Solution of the Distribution of Stress Intensity Factor Along the Front of a 3D Rectangular Crack by Using a Singular Integral Equation Method," Trans. Jpn. Soc. Mech. Eng., Ser. A, **66**(650), pp. 1922–1927 (in Japanese).
[11] Chen, M. C., and Tang, R. J., 1997, "An Explicit Tensor Expression for the Fundamental Solutions of a Bimaterial Space Problem," Appl. Math. Mech., **18**(4), pp. 331–340.
[12] Erdogan F., 1978, "Mixed Boundary Value Problems," *Mechanics Today*, S. Nemat-Nasser ed., Pergamon Press, New York, **4**, pp. 1–86.
[13] Tang, R. J., and Qin, T. Y., 1993, "Method of Hypersingular Integral Equations in Three-Dimensional Fracture Mechanics," Acta Mech. Sin., **25**, pp. 665–675.
[14] Qin, T. Y., and Tang, R. J., 1993, "Finite-Part Integral and Boundary Element Method to Solve Embedded Planar Crack Problems," Int. J. Fract., **60**, pp. 191–202.
[15] Noda, N. A., and Wang, Q., 2000, "Application of Body Force Method to Fracture and Interface Mechanics of Composites," Research Report of the JSPS Postdoctoral Fellowship for Foreign Researchers, No. 98187.
[16] Isida, M., Yoshida, T., and Noguchi, H., 1991, "A Rectangular Crack in an Infinite Solid, a Semi-Infinite Solid and a Finite-Thickness Plate Subjected to Tension," Int. J. Fract., **52**, pp. 79–90.